Reduction of Leakage Currents in Silicon Mesa Devices

Reinhart D. Kühne and Erich Kasper

***Abstract*— Easily and rapidly manufacturable silicon mesa devices suffer from additional leakage currents from the mesa rim where n-p junctions are exposed to the surface. A modified mesa structure is proposed, which reduces the drawbacks of leakage currents. The structure contains a metallization smaller than the mesa and a very thin (10-nm) contact layer as, for instance, can be grown by molecular beam epitaxy (MBE). The current distribution for a forward-biased junction is given. For cylindrical symmetry, it was possible to derive analytical solutions. At high current densities, the voltages at the mesa edge are effectively reduced and the current contribution of the outer part is only a small fraction of the total current. Numerical examples are given for large test structures as used for microwave IMPATT diodes.**

***Index Terms*—Current modeling, IMPATT diode, mesa structure.**

I. Introduction

Millimeter-wave devices have typical active region lengths of 30–100 nm, depending on whether diffusive transport or drift transport dominates. The diffusion width and drift width can be estimated to be [1]

$$\text{diffusion width:} \quad L_{\text{Diff}} = (D \cdot \tau)^{1/2} \quad \sim 30 \text{ nm} \tag{1}$$

$$\text{drift width:} \quad L_{\text{Drift}} = v_s \cdot \tau \quad \sim 100 \text{ nm.} \tag{2}$$

For the assessment $D = 10^{-3}$ m^2/s was chosen, which is a common value in doped material, and $v_s = 10^5$ m/s and $\tau = 10^{-12}$ s for 100-GHz operation, respectively. Often, these very thin active regions are grown by advanced epitaxy methods based on vapor phase epitaxy (VPE) or molecular beam epitaxy (MBE). In order to obtain a fast device, all parasitic elements have to be suppressed as not to mask the intrinsic speed of the device. Planar technology, self-adjusted contacts, and surface passivation deliver reliable, but technically cumbersome, solutions with long development cycles. For first assessments, large-area test structures, which are producible in small-volume production lines, were chosen. With respect to these requirements, mesa devices are preferred, however, enhanced breakdown and leakage currents across exposed n–p junctions may be a serious problem. Especially for devices operated under high-power densities, the rather unpredictable conditions at the mesa edge may cause lifetime problems or noisy operation. Typical silicon microwave devices which operate under high-power densities are IMPATT diodes (breakdown regime) or SiGe heterobipolar transistors (HBT's) driven for high-speed operation up to the onset of the Kirk effect.

We propose a mesa-like device configuration which exploits the benefits of mesa devices, namely, easy fabrication and rapid tests, without being plagued by the drawbacks of severe leakage currents from the rim. The ingredients of the proposal are: 1) a contact metallization much smaller than the mesa and 2) an extremely thin, but highly doped contact layer beneath the semiconductor/metal interface. Such layers, e.g., 10-nm thick with doping concentrations above 10^{19} cm^{-3}, can be grown by advanced methods like MBE

Manuscript received October 21, 1997; revised February 16, 1998.
R. D. Kühne is with Steierwald Schonharting and Partner GmbH, D-70565 Stuttgart, Germany (e-mail: ssp@ssp-s.ccmail.compuserve.com).
E. Kasper is with the Institut für Halbleitertechnik, Universität Stuttgart, D-70565 Stuttgart, Germany.
Publisher Item Identifier S 0018-9480(98)03445-0.

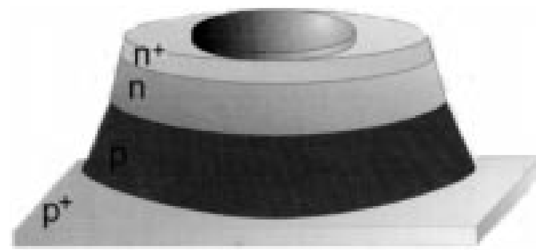

Fig. 1. n–p IMPATT diode as mesa structure with confined current distribution.

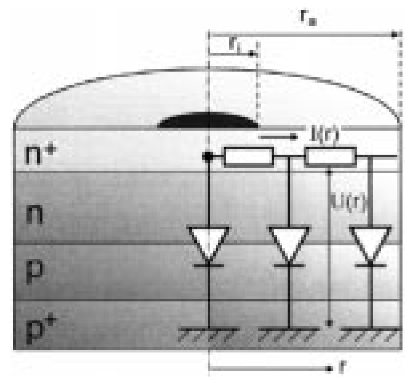

Fig. 2. Equivalent circuit of the mesa device of Fig. 1.

[2], but are hardly available with more usual production methods. The sheet resistivity $R_s = 1/(\sigma d) = 1/(en\mu d)$ of the contact layer may be between 10^3–10^5 Ω.

The specific contact-layer design provides good contact resistance because of high doping, low series resistance because of low thickness, and high spreading resistance for in-plane currents because of the sheet resistivity. Fig. 1 shows the now proposed mesa-device structure. The current confinement is obtained by an inner-area metallization and by the specific contact layer with high sheet resistance, which suppresses the outspread of current to the outer n-p-junction elements. Simply speaking, the highly unpredictable edge effect is replaced by a predictable parasitic element, whose influence even decreases at higher frequencies because of the *RC* load. Consider only for illustration a 1 μm $\times$ μm diode element 5 μm outside the metal contact with 50-kΩ series resistance and 2-fF capacitance resulting in 2-GHz cutoff.

For convenience, a simple n-p diode is considered in Fig. 1, but it can be applied to contacts of a variety of device structures. The leakage currents I_ℓ from the rim of the mesa roughly follow an I–V characteristics that is typical for recombination currents in the forward direction

$$I_\ell = I_{\ell 0} \exp[U_a/(2U_T)] \tag{3}$$

with U_a being the voltage difference across the space charge layer (SCL) at the rim, $U_T = 25$ mV thermal voltage at room temperature, and $I_{\ell 0}$ leakage saturation current, which is slightly dependent on the voltage. We neglect this dependence here. From (3), it immediately follows that the leakage current is strongly reduced when the voltage U_a is reduced. This is the case in the modified structure. The leakage current from the mesa rim, for instance, will be reduced by a factor of

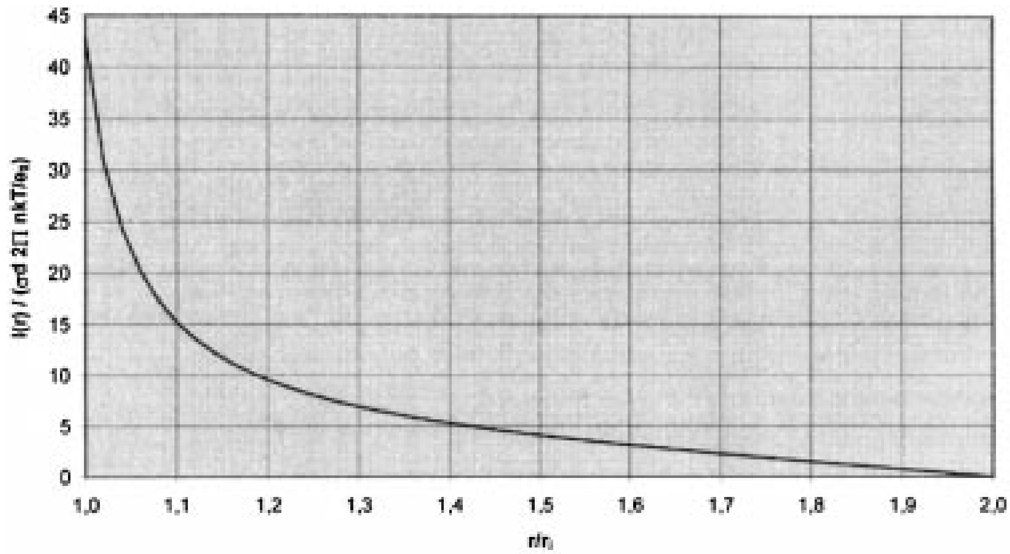

Fig. 3. Spreading current $I(r)$ against the radius for the ratio (for parameters used, see Table I with $U_i = 0.94$ V).

100 when U_a is reduced by 130 mV. In the following, we calculate the current distribution for a forward fixed junction in the modified mesa structure. For cylindrical symmetry, analytical solutions of the nonlinear differential equation are given.

II. Model Equations and Solutions

The complete structure, as shown in Fig. 1, is characterized as follows: the top layer can be considered as a circuit-layer resistance with the specific resistance of the top layer and the connected elements of diodes, which are interconnected by the relationship of current voltage and flux density, corresponding to a usual n-p junction. The equivalent circuit is sketched in Fig. 2.

With this equivalent-circuit presentation, the model equations read

$$I = \sigma d 2\pi r \left(-\frac{dU}{dr}\right) \tag{4}$$

if Ohm's law is applied to the radial distribution of the current, and

$$\frac{dI}{dr} = -2\pi r j[U(r)] \tag{5}$$

as an ansatz to the continuous radial decrease of the current. This is due to the connection of the sinks caused by the n-p junctions in the lower top layer. If an exponential characteristic as a relation between current–density and voltage

$$j = j_0 e^{U/(nkT/e_0)} \tag{6}$$

is used, the model equation for the distribution of the radial voltage can be simplified in dimensionless variables to

$$\frac{1}{\hat{r}}\frac{d}{d\hat{r}}\left(\hat{r}\,\frac{d\hat{U}}{d\hat{r}}\right) - 2ae^{\hat{U}} = 0$$
$$\hat{r} = \frac{r}{r_a}$$
$$\hat{U} = \frac{U}{nkT/e_0} = \frac{U}{nU_T}. \tag{7}$$

The model equation thus contains only the model parameter a

$$a = \frac{1}{2}\,\frac{j_o r_a^2}{nkT/e_0}\,\frac{1}{\sigma d} = \frac{I_0 \cdot R_s}{nU_T}\,\frac{r_a^2}{r_i^2} \tag{8}$$

describing the current–voltage characteristic.

The equations are solved with respect to appropriate boundary conditions. These are the voltage at the contact

$$U(r = r_i) = U_i$$

and the vanishing of the electric current at the boundary

$$I \sim \frac{dU}{dr} = 0 \text{ at } r = r_a.$$

The complete solution is found by using the transformation $x = \ln \hat{r}$, $V = U + 2x$, which leads to the concise representation transformation

$$V'' = 2ae^{V}. \tag{9}$$

Adapting the boundary conditions, voltage and current distribution can be found from (9)

$$\hat{U}(x) = \hat{U}_a - 2x - 2\ln|v|$$
$$v = \begin{cases} \cos\left[\sqrt{p^2-1}(-x)\right] + \dfrac{\sin\left[\sqrt{p^2-1}(-x)\right]}{\sqrt{p^2-1}}, & p > 1 \\ 1-x, & p = 1 \\ \cosh\left[\sqrt{1-p^2}(-x)\right] + \dfrac{\sinh\left[\sqrt{1-p^2}(-x)\right]}{\sqrt{1-p^2}}, & p < 1 \end{cases} \tag{10}$$

with $p^2 = ae^{U_a/nU_T}$.

III. Current Distribution and I–V Characteristic

The physical dimensions, the characteristic parameters, as well as the characteristics of the IMPATT diode chosen for the numerical calculations are listed in Table I.

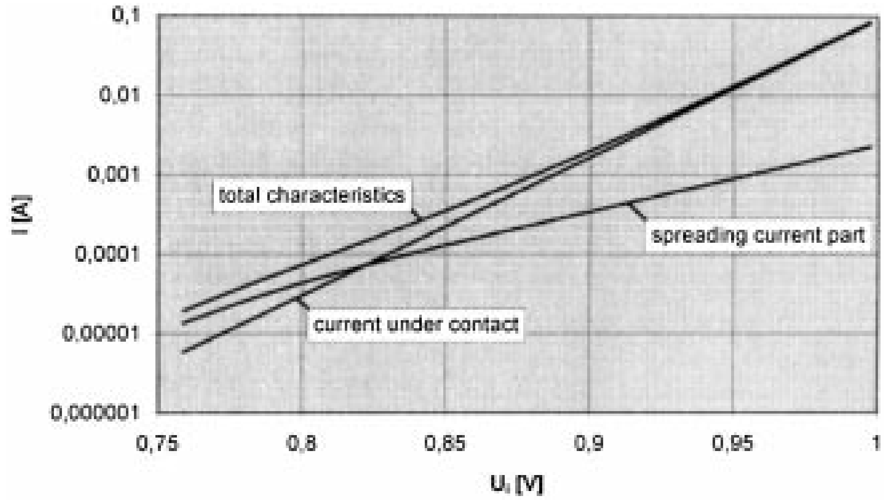

Fig. 4. Characteristic line $I = I(U_i)$ for the total current, the current part below the contact area, and the spreading current part. (For parameters used, see Table I.)

TABLE I
APPLIED DIMENSIONS AND CHARACTERISTIC VALUES

Contact spot	r_i	=	35 µm
Mesa radius	r_a	=	70 µm
Sheet resistance	$R_s = 1/(\sigma d)$	=	10100 Ω
Applied voltage (forward)	U_i	=	0.75 - 1.0 V
Diode characteristics	j	=	$j_0\ e^{\frac{U}{n_0 kT/e0}}$
	j_0	=	$10^{-10}\ \frac{A}{m^2}$
	n	=	1
	$U_T = kT/e_0$	=	25mV

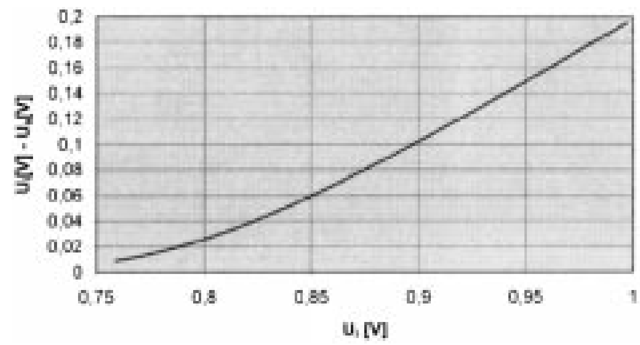

Fig. 5. Difference between applied voltage U_i and boundary voltage U_a as a function of the applied voltage U_i.

The distribution of the spreading electrical current $I(r)$—as given in Fig. 2 in dependence of the radius r based on (10)—is shown in Fig. 3.

The figure shows the rapid decay of the electric current with increasing distance from the center contact of the device. The high lateral sheet resistance of the thin contact layer in conjunction with the nonlinear vertical current density characteristics suppresses effectively the otherwise possible outspreading of current from the center contact.

As characteristics, the relation between the total electric current through the n-p junction and the applied voltage are given. This leads to

$$I_{\text{total}} = f(U_i) = \pi r_i^2 j_0 e^{U_i/(nkT/e_0)} + I(r_i). \qquad (11)$$

Fig. 4 shows both parts (current under contact area, spreading current part) which compose the total current characteristics, and the total current characteristics I_{total}.

With increasing current, the contribution of the spreading current to the outer area $A_a = \pi(r_a^2 - r_i^2)$ monotonically decreases. With 10-mA total current, the spreading part is 20% which is decreasing to 2% in case of a total current of 100 mA, although the outer area is three times larger than the contact area in this specific example. The results can also be interpreted by a concentrated equivalent circuit where the outer area is described by a diode with area A_a connected to a single series resistance $R_a(U_i)$

$$I(r_i) = A_a j_0 \ \exp\left[\frac{U_i - R_a \cdot I(r_i)}{nU_T}\right]. \qquad (12)$$

IV. DISCUSSION

The current contribution and the resulting voltage at the mesa rim can be effectively reduced by the modified mesa structure. This is shown for forward biased junctions and for the relatively large mesa structures with circular geometry. Fig. 5 shows the voltage difference $(U_i - U_a)$ as function of the applied voltage U_i. With increasing voltage and, therefore, exponentially increasing current, the resulting voltage at the rim U_a drops significantly below the applied voltage. Compared to conventional mesa structures, leakage currents from the rim will be considerably reduced.

How may these results be generalized? The spreading resistance effect of the thin contact layer works whenever a nonlinear device characteristics is driven to high current densities. In reverse-biased silicon IMPATT diodes [5], this happens when avalanche multiplication onsets. The modified structure suppresses highly nonreproducible multiplication at the rim and could, therefore, improve reproducibility and lifetime of integrated IMPATT diodes in silicon monolithic millimeter-wave integrated circuits (SIMMWIC's) [6]. Also with advanced SiGe/Si hetero devices [7], [8], the modified mesa may be applied to provide test structures with reduced leakage currents.

The given results concern dc characteristics, but it is obvious that the resistive effect of the thin contact layer is even more effective under RF operation when capacitive currents are added. A detailed study of RF effects will follow later.

The calculations are performed for rather large test structures. A reduction of the device structures would reduce the benefits when not increasing sheet resistance, which needs some technological efforts.

REFERENCES

[1] S. M. Sze, *Physics of Semiconductor Devices.* New York: Wiley, 1981.

[2] E. Kasper and J. C. Bean, *Silicon Molecular Beam Epitoxy.* Boca Raton, FL: CRC Press, 1988.

[3] R. Kühne and E. Kasper, "Berechnung der Stromverteilung für die Stromzutuhr für Mikrowellenheterobauelemente," *Tagung des U.R.S.I.-Landesausschusses in der Bundesrepublik Deutschland und der ITG Fachausschüsse Kleinheubach*, Oct. 2–6, 1995; *Kleinheubacher Berichte*, vol. 39, pp. 41–50, 1996.

[4] R. Kamke, *Gewöhnliche Differentialgleichungen.* Berlin, Germany: Springer-Verlag, 1983.

[5] J.-F. Luy and R. Kühne, "Tunneling assisted IMPATT operation," *IEEE Trans. Electron Devices*, vol. 36, pp. 589–595, Mar. 1989.

[6] J.-F. Luy and P. Russer, *Silicon Based Millimeter Devices.* Berlin, Germany: Springer-Verlag, 1994.

[7] E. Kasper, "Silicium germanium heterodevices," *Appl. Surface Sci. 102*, pp. 189–193, 1996.

[8] ____, "SiGe Alloys and heterojunctions—Extending the performance of Si devices," *Current Opinion Solid State Material Sci.*, vol. 2, pp. 48–53, Feb. 1997.